Characterization of gravitational-wave burst polarizations with the BayesWave algorithm

THE UNIVERSITY OF MELBOURNE

OzGrav
ARC Centre of Excellence for Gravitational Wave Discovery

Yi Shuen C. Lee, Meg Millhouse, Andrew Melatos

CHRISTINE LEE
ylee9@student.unimelb.edu.au
@AstroOrca

INTRODUCTION

The global gravitational-wave (GW) detector network currently consists of four interferometers: LIGO Hanford (H) and Livingston (L), Virgo (V) and KAGRA (K); the commissioning of LIGO India is also well underway. The expanding detector network enables more accurate probing of GW polarizations, as each detector measures the combination of polarization states independently. *BayesWave* [1] is a source-agnostic analysis pipeline designed for the joint detection and characterization of GW transients (i.e. bursts) and instrumental glitches. In this work, we present a multi-detector analysis on *BayesWave*'s ability to (i) detect and characterize GW signals from precessing and non-precessing binaries and (ii) recover polarization content of GW bursts.

BAYESWAVE RECONSTRUCTION

BayesWave reconstructs transient, non-Gaussian features in the data as a sum of sine-Gaussian wavelets. Signal models in earlier versions of *BayesWave* are restricted to elliptical polarizations ($\mathbf{E}$):

$$\tilde{h}_+ = \sum_n^N \Psi(f; t_0^n, f_0^n, Q^n, A^n, \phi_0^n)$$
$$\text{with } \tilde{h}_\times = i\epsilon\tilde{h}_+$$

where ϵ encodes the degree of elliptical polarization; Ψ denotes sine-Gaussian wavelets; N is the total number of wavelets; and the n-th wavelet is parameterized by: central time t_0, central frequency f_0, quality factor Q, amplitude A and phase ϕ_0. In a recent update [2], *BayesWave* relaxes the elliptical constraint to optimize the characterization of unpolarized signals like white noise bursts and supernova. This relaxed polarization model ($\mathbf{R}$) allows $\tilde{h}_+$ and $\tilde{h}_\times \neq i\epsilon\tilde{h}_+$ to be reconstructed independently, while assuming the same N, t_0^n, f_0^n and Q^n for both polarization states [2].

GW STOKES PARAMETERS

Polarization content of a monochromatic plane wave is typically encoded in terms of Stokes parameters; for polychromatic GW signals, the Stokes parameters are a function of frequency. *BayesWave* assumes purely tensorial polarizations as predicted by GR, in which case the Stokes parameters are given by [3]

$$I = |\tilde{h}_+|^2 + |\tilde{h}_\times|^2 \qquad Q = |\tilde{h}_+|^2 - |\tilde{h}_\times|^2$$
$$U = \tilde{h}_+\tilde{h}_\times^* + \tilde{h}_\times\tilde{h}_+^* \qquad V = i(\tilde{h}_+\tilde{h}_\times^* - \tilde{h}_\times\tilde{h}_+^*)$$

As in electromagnetism, I describes the total intensity, $\mathbf{L} = \sqrt{Q^2 + U^2}/I$ measures the degree of linear polarization (i.e. preponderance of $\tilde{h}_+$ over $\tilde{h}_\times$), $\mathbf{C} = V/I$ measures the degree of circular polarization and $\mathbf{T} = \sqrt{\mathbf{L}^2 + \mathbf{C}^2}$ measures the total polarized fraction of the signal (as opposed to unpolarized).

INJECTION SETS

- IMRPhenomXPHM - Phenomenological binary black holes (BBH) [4]
- 200 events, Component masses: $40 - 8M_\odot$, Uniform sky location, Fixed initial inclination at 45°
- **Set (1)** Zero-spin, **non-precessing binaries**, and **Set (2)** Spin-enabled, **precessing binaries**, where the initial dimensionless spin $\vec{\chi}$ for each component mass is independently sampled within $0.1 \leq |\vec{\chi}| \leq 1.0$

BAYES FACTOR - ELLIPTICAL (E) vs. RELAXED (R)

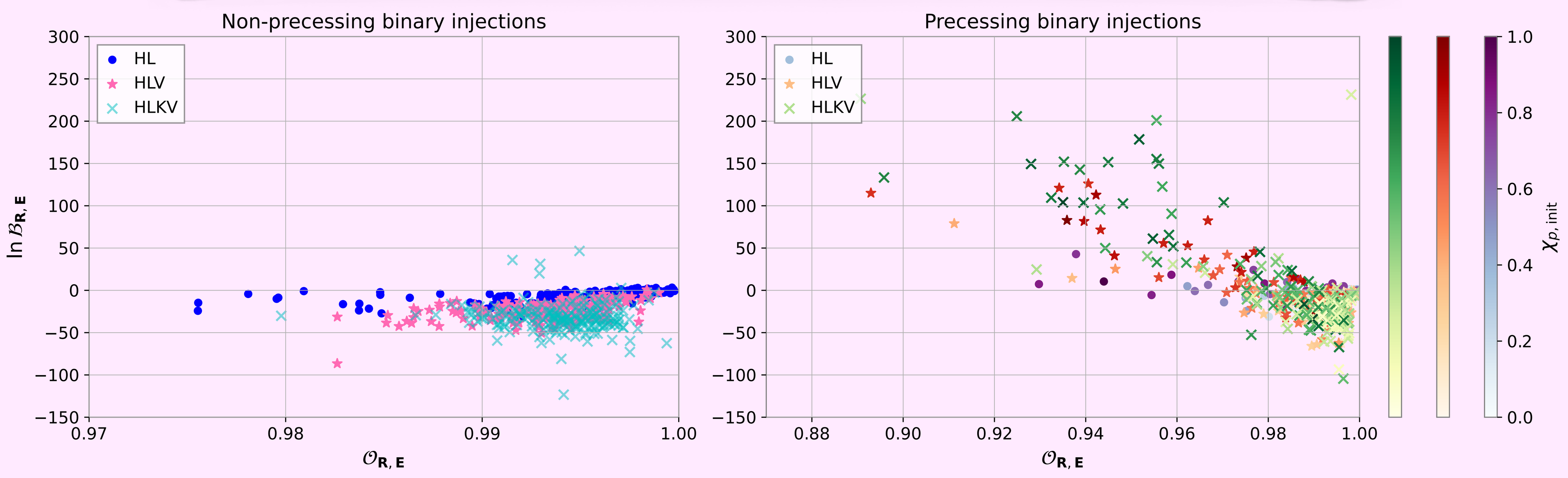

Fig. 1 - **Log Bayes factor** between $\mathbf{R}$ and $\mathbf{E}$ ($\ln \mathcal{B}_{\mathbf{R,E}}$) versus the **Waveform overlap** between $\mathbf{R}$ and $\mathbf{E}$ ($\mathcal{O}_{\mathbf{R,E}}$). The color bars indicate the *initial* spin-precession parameter $\chi_{p,\mathrm{init}}$ [5] for the precessing binaries (right panel). All non-precessing binaries (left panel) have $\chi_p = 0$ throughout the inspiral. Injections that are consistent with the glitch or Gaussian-noise models are excluded from this analysis.

To understand how *BayesWave*'s model selection and signal reconstruction benefits from $\mathbf{R}$ and with additional detectors, we plot $\ln \mathcal{B}_{\mathbf{R,E}}$ vs. $\mathcal{O}_{\mathbf{R,E}}$ for the HL, HLV and HLKV networks as in Fig. 1. More positive $\ln \mathcal{B}_{\mathbf{R,E}}$ indicates more evidence for $\mathbf{R}$ compared to $\mathbf{E}$, and vice versa; higher overlap $\mathcal{O}_{\mathbf{R,E}}$ indicates more agreement (match) between the $\mathbf{R}$ and $\mathbf{E}$ waveforms. For **non-precessing binaries** (left panel), there is no obvious trend between $\ln \mathcal{B}_{\mathbf{R,E}}$ and $\mathcal{O}_{\mathbf{R,E}}$. While all events are recovered with $\mathcal{O}_{\mathbf{R,E}} > 0.97$, the bulk of $\mathcal{O}_{\mathbf{R,E}}$ shifts closer to unity with reducing spread as the detector network expands, i.e. $\mathbf{R}$ and $\mathbf{E}$ reconstructions become increasingly similar with additional detectors. Consequently, $\ln \mathcal{B}_{\mathbf{R,E}}$ becomes more negative, favouring $\mathbf{E}$. This is because the evidence of $\mathbf{R}$ is penalized by the Occam factor for its unnecessarily larger parameter space. For **precessing binaries** (right panel), the $\ln \mathcal{B}_{\mathbf{R,E}}$ becomes more positive for \, that is when $\mathbf{R}$ and $\mathbf{E}$ reconstructions deviate further from one another. This is generally observed in events with higher $\chi_{p,\mathrm{init}}$, where the presence of in-plane spin leads to orbital plane precession and signal amplitude modulations that cannot be modelled by $\mathbf{E}$. The $\ln \mathcal{B}_{\mathbf{R,E}}$ also becomes increasingly positive with larger detector networks, because information from additional detectors also enables $\mathbf{R}$ to capture both the modulations and non-elliptical polarization structure of the signal more accurately.

STOKES PARAMETER RECOVERY

We define the match ($\mathcal{M}$) analogous to standard LIGO-Virgo KAGRA definition of overlap ($\mathcal{O}$) [6], to quantify the similarity between the injected (inj) and recovered (rec) polarization fractions, $\mathbf{P} \in \{\mathbf{L}, \mathbf{C}, \mathbf{T}\}$ in the frequency domain:

$$\mathcal{M}_{\mathbf{P}} = \frac{\langle \mathbf{P}_{\mathrm{inj}}, \mathbf{P}_{\mathrm{rec}} \rangle}{\sqrt{\langle \mathbf{P}_{\mathrm{inj}}, \mathbf{P}_{\mathrm{inj}} \rangle \langle \mathbf{P}_{\mathrm{rec}}, \mathbf{P}_{\mathrm{rec}} \rangle}}, \text{ with } \langle a, b \rangle = \int_{f_{\mathrm{low}}}^{f_{\mathrm{high}}} ab^* \, df.$$

$\mathbf{P} \in \{\mathbf{L}, \mathbf{C}, \mathbf{T}\}$ are real quantities, thus $b = b^*$. To optimally assess the accuracy of *BayesWave* in recovering polarization content, we set the frequency range of our analysis to $f_{\mathrm{low}} = 40\,\mathrm{Hz}$ and $f_{\mathrm{high}} = 400\,\mathrm{Hz}$, which is where GW detector noise floors are lowest. In Fig. 2 we compare $\mathcal{M}_{\mathbf{P}}$ of the **HL** and **HLKV** networks against **HLV**, for the **precessing binary injections**. The $\mathcal{M}_{\mathbf{P}}$ for **HL** injections (in purple) are generally lower than **HLV** for all $\mathbf{P} \in \{\mathbf{L}, \mathbf{C}, \mathbf{T}\}$; the converse is true for **HLKV** (in green). This suggests that larger detector networks increases *BayesWave*'s precision in recovering polarization content. However, we note that $\mathcal{M}$ of $\mathbf{L}$ is generally lower than $\mathbf{C}$ and $\mathbf{T}$. This is because polarization of binary coalescences GW signals are predominantly circular and therefore lack signal power in the linear configuration (unless viewed edge-on i.e. 90° inclination).

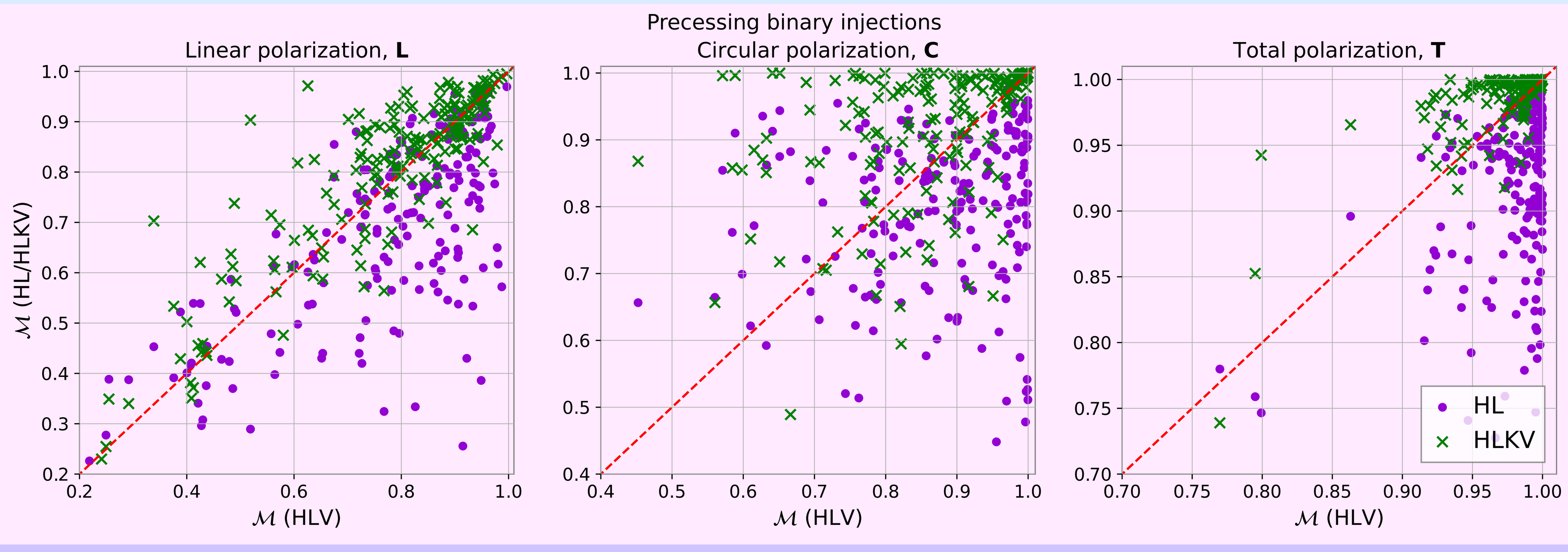

Fig. 2 - $\mathcal{M}_{\mathbf{P}}$ comparisons: **HL** (purple circles) / **HLKV** (green crosses) versus **HLV**. The diagonal line indicates equal $\mathcal{M}_{\mathbf{P}}$ for both detector networks on the horizontal and vertical axes.

KEY TAKEAWAYS

We assess *BayesWave*'s ability to characterize GW bursts with the relaxed polarization model $\mathbf{R}$, using simulated precessing and non-precessing BBH signals. We compare $\ln \mathcal{B}_{\mathbf{R,E}}$ for the two types of BBH and find increasing evidence for $\mathbf{R}$ with precessing BBHs, when $\mathbf{R}$ and $\mathbf{E}$ reconstructions deviate further from one another. The increasing evidence is especially prominent with larger detector networks. We also show that larger networks recover polarization fractions more accurately, using $\mathcal{M}$ as the metric. As the global detector network continues to expand, there is a promising outlook for *BayesWave* in (i) the characterisation and detection of precessing binaries and (ii) more accurately probing the polarization content of GW bursts with $\mathbf{R}$.

This material is based upon work supported by the LIGO Laboratory fully funded by the National Science Foundation.

[1] N. Cornish and T. Littenberg, Class. Quantum Grav. 32, 135012 (2015).
[2] N. Cornish et al., Phys. Rev. D 103, 044006 (2021).
[3] J. Romano and N. Cornish, Living Rev Relativ 20, 2 (2017).
[4] G. Pratten et al., Phys. Rev. D 103, 104056 (2021).
[5] P. Schmidt et al., Phys. Rev. D 91, 024043 (2015).
[6] R. Abbott et al., Phys. Rev. X 11, 021053 (2021).

LIGO VIRGO KAGRA